CALCULATION OF THE FLOW FIELD IN AN AXIAL FAN WITH VARIABLE SWIRL DISTRIBUTION AT OFF-DESIGN OPERATING POINTS

Patrick VOGEL, Matthias SEMEL, Antonio DELGADO

Institute of Fluid Mechanics (LSTM)
Friedrich-Alexander University Erlangen-Nuremberg
Cauerstraße 4, 91058 Erlangen, Germany

SUMMARY

A novel procedure has been modelled and implemented with the aim to enable precise calculations of the off-design flow field in an axial fan accounting for the existence of curved meridional streamlines. This is achieved by combining off-design radial equilibrium calculations, the streamline curvature method and the surface vorticity method. The written program is used to calculate the head curves and velocity components of a reference fan for a specified range of operating points. Results of the implementation are validated by comparison with CFD simulations and found to be in good agreement.

INTRODUCTION

The preliminary design of axial fans is usually performed at a specified design point. In an inverse design approach, a suitable work distribution is chosen to fulfill the design requirements and the necessary blade angles are determined. In most cases, the chosen work distribution is affecting the flow field behind the axial fan and the meridional velocity component of the absolute velocity becomes a function of the radius. The flow field can then be characterized as a radial equilibrium flow. The next step in the design process is often performed by a combination of S1 and S2 calculations in order to model the flow inside the blade channel. There are different approaches, which include viscous and potential effects of the blade geometry on the flow field. Nevertheless, most of these approaches need a fixed blade geometry and thus the solutions is based on a direct approach. Most inverse approaches are neglecting the effect of the curved streamlines and are calculating the cascade solution on radial cross section. In order to improve the quality of a full inverse design a calculation method is necessary which respects the differences occurring due to the chosen work distribution not depending on an actual fixed blade geometry. The presented method aims at closing this gap.

The present communique takes advantages of a previously presented method to predict the ideal flow field of an axial fan at design and off-design. A one way coupled calculation method is presented to calculate the ideal hydraulic characteristic and the flow field of an axial fan at any operating condition. The ideal flow field is calculated at any flow rate by the help of a streamline curvature method. In a next step, a potential cascade solution is calculated on curved streamlines fitting to the actual streamline distribution at the actual working point.

In the presented work, the authors will design a fan with a constant reaction work distribution. The ideal hydraulic characteristic and the flow field of the designs will then be calculated by the help of the proposed method. The real flow features will be derived by RANS CFD. The derived characteristics and the flow fields will be compared with the theoretical ones and the application range of this approach will be determined.

METHODS AND MATERIALS

Throughout this chapter, the flow within the fan will be assumed to be stationary, incompressible, axisymmetric, inviscid and loss-free. The reader is referred to the annex for the nomenclature of the variables.

Streamline Curvature Method

Developed in the 1960s, the streamline curvature (SLC) method offers a relatively simple and efficient way for calculating the two-dimensional streamline pattern inside a turbomachine on the S2 (meridional) plane. It is an iterative numerical procedure, based on the alternating fulfilment of both the radial momentum equation and the continuity equation where the results of each are used to correct the starting conditions of the other, respectively, until a convergence criterion is reached. With the simplifications mentioned above, the radial equilibrium equation is

$$c_r \frac{\partial c_r}{\partial r} + c_z \frac{\partial c_r}{\partial z} - \frac{c_\theta^2}{r} = -\frac{1}{\rho}\frac{\partial p_s}{\partial r} + F_r \qquad (1)$$

The SLC method makes use of the meridional direction m which follows the direction of the streamline and the corresponding velocity component c_m. With this and after performing some transformations [8], eq. (1) can be rewritten as

$$c_m \frac{\partial c_m}{\partial r} = c_m \frac{\partial c_m}{\partial m}\sin\phi - c_m^2 \frac{\cos\phi}{r_c} + \frac{\partial h_t}{\partial r} - T\frac{\partial s}{\partial r} - \frac{c_\theta}{r}\frac{\partial (r c_\theta)}{\partial r} - \sin\phi\, F_m - \cos\phi\, F_n \qquad (2)$$

Eq. (2) is the governing equation that is to be solved by the SLC procedure. The term $T\frac{\partial s}{\partial r}$ vanishes due to the assumption of loss-free flow. According to HEARSEY [9], the computation is made easier if eq. (2) is rewritten to another form through further transformations, thereby eliminating the term $c_m \frac{\partial c_m}{\partial m}\sin\phi$. The resulting equation is quite lengthy and will thus not be shown explicitely here; the reader is referred to the literature for details.

It is to be noted that the solution of eq. (2) requires the prescription of a radial swirl distribution rc_θ along the fan blades. This can be done easily for conditions at the design point of the machine. At off-design conditions, however, where the volume flow ratio

$$\chi = \frac{Q_{op}}{Q_{des}} \qquad (3)$$

does not equal one, a considerable amount of additional calculations is necessary to obtain the actual $c_{\theta 3}$ values behind the rotor. This has been the subject of the work of SEMEL [3] who presented an

analytical method for calculating the $c_{\theta 3}$ and c_{z3} downstream of the rotor under radial equilibrium flow conditions as follows:

$$c_{\theta 3}(r,\chi) = r\omega(\psi + (\chi - 1) \cdot \Delta c_\theta) \tag{4}$$

$$c_{z3}(r,\chi) = c_{z3}(r,\chi = 1) \cdot (1 + (\chi - 1)\Delta c_z) \tag{5}$$

, where

$$\Delta c_\theta = (\psi - 1) C Q_{des} \prod_{i=1}^{n} (r - r_i)^{-\frac{1}{1+\psi(r_i)}} \tag{6}$$

$$\Delta c_z = C Q_{des} \prod_{i=1}^{n} (r - r_i)^{-\frac{1}{1+\psi(r_i)}} \tag{7}$$

Details regarding eqs. (4) to (7) are to be taken from [3]. An existing MATLAB implementation was used to calculate the SLC input swirl distribution $rc_{\theta 3}$, whereas the c_{z3} results were later used for comparison to the c_m results obtained by the SLC method.

The application of the SLC method to grid points inside the bladed region needs some particular attention due to the far more complex flow field. This might be a reason why the common applications of the SLC method seem to be limited to the region outside the rotor. In the present work, however, S2 streamline shapes are explicitly required across the blades, which is why the present implementation features some computing stations in relatively short axial intervals. The spacing has to be chosen carefully as it might be detrimental to convergence and/or runtime of the program. Since the exact development of the c_θ profile in the blade passage cannot be predicted at this point, it is assumed to increase linearly from $c_{\theta 1}$ (blade inlet) to $c_{\theta 2}$ (blade outlet). For the inlet region, swirl-free inflow is assumed so that $c_{\theta 1} = c_{\theta 0} = 0$ and for the outlet region, loss-free conservation of swirl is assumed so that $c_{\theta 2} = c_{\theta 3}$.

The steps of the SLC program have been described in detail by a multitude of authors [7][8][9]. In short, they are:

1. Definition of axial stations and initial streamlines
2. Computation of streamline slope and curvature
3. Calculation of $c_m(r)$ profile from eq. (2) with initial c_m guess at present axial station
4. Check of integrated mass flow over channel section with $c_m(r)$; if continuity is not fulfilled: iterate from step 3 with corrected c_m guess
5. Shift radial positions of streamlines until mass flow is equal between adjacent streamlines; proceed to next axial station when finished
6. Check overall streamline shift and end program if tolerance is reached; otherwise iterate from step 2

Surface Vorticity Method for Airfoils

The surface vorticity method as described and reviewed in detail by LEWIS [4][5] enables numerical calculation of the two-dimensional flow field around single airfoils and airfoil cascades. It has also been thoroughly reviewed and applied by SMITH [1][2] who provided the basis for this part of the present work.

In a viscous flow, the decrease of velocity towards a wall generates vorticity in said area. In an inviscid flow, however, no such velocity gradient will exist, which means that the vorticity will be generated in an infinitesimally thin sheet across which the flow velocity c drops from its far-field value c_∞ to zero. It can be shown that the surface velocity c_s tangential to the profile outline is equivalent to the local vorticity strength $\gamma(s)$ generated in the vorticity sheet:

$$c_s = \gamma(s) \tag{8}$$

To satisfy the condition $c = 0$ inside the profile, the vorticity sheet has to move itself along the surface at the speed $\frac{1}{2}\gamma(s)$. Application of the described method to a two-dimensional body immersed in a flow field given by a relative far-field velocity w_∞ and an angle of attack α yields

$$-\frac{1}{2}\gamma(s_i) + \oint k(s_i, s_j)\gamma(s_j)ds_j + w_\infty(\cos\alpha\cos\vartheta_i + \sin\alpha\ \sin\vartheta_i) = 0 \tag{9}$$

Eq. (9) describes the influence of the local vortex strength given by $\gamma(s_j)ds_j$ at a point j of the profile outline on the velocity components at another location i, where ϑ_i stands for the local slope angle of the outline relative to the x-axis and $k(s_i, s_j)$ is a geometrical coupling coefficient.

In order to perform a numerical solution for the surface velocity c_s, discretization of the outline into M finite panels is required. Eq. (9) then becomes

$$\sum_{j=1}^{M} K(s_i, s_j)\gamma(s_j) = -w_{x\infty}\cos\vartheta_i - w_{y\infty}\sin\vartheta_i \tag{10}$$

The new coupling coefficients $K(s_i, s_j)$ are given by

$$K(s_i, s_j) = K_{ij} = \frac{\Delta s_j}{2\pi}\left(\frac{(y_i - y_j)\cos\vartheta_i - (x_i - x_j)\sin\vartheta_i}{(x_i - x_j)^2 + (y_i - y_j)^2}\right) \tag{11}$$

for $i \neq j$. For $i = j$, further calculations are required which eventually yield

$$K(s_i, s_i) = K_{ii} = -\frac{1}{2} - \frac{1}{8\pi}(\vartheta_{i+1} - \vartheta_{i-1}) \tag{12}$$

With eqs. (11) and (12), the equation system (10) is now defined and can be solved numerically to obtain the vector $\gamma(s)$ which, according to eq. (8), yields the values of surface velocity c_s on each of the M previously defined panels of the profile outline.

However, the surface vorticity method exhibits some peculiarities when applied to airfoils due to their thin shape. In order to prevent residual circulation inside the profile, a back-diagonal correction has to be applied to the coupling matrix K_{ij}, making it singular. This can be avoided by adding the bound circulation to the right-hand side of eq. (10). The bound circulation can be calculated from the Kutta condition which states that the absolute values of c_s must be equal at the panels adjacent to the trailing edge of the airfoil, which also implies the use of a sharp trailing edge. This is provided by NACA profiles which also offer the advantage of a possible inverse calculation of the profile geometry in order to match prescribed relative flow angles β_2 and β_3; see Smith [1] for details.

The surface vorticity method can be extended from the single airfoil to an infinite airfoil cascade by using the theory of TRAUPEL [6] which accounts for the blade spacing t. The corresponding equations for the new coupling coefficients and the velocity components throughout the entire flow field outside the profile outlines then become, respectively,

$$K_{ij} = \frac{\Delta s_j}{2\pi}\left(\frac{(y_i - y_j)\cos\vartheta_i - (x_i - x_j)\sin\vartheta_i}{(x_i - x_j)^2 + (y_i - y_j)^2}\right) \tag{13}$$

$$c_x(x, y) = w_{x\infty} + \sum_{j=1}^{M}\frac{\gamma(s_j)\Delta s_j}{2t}\left(\frac{\sin\left[\frac{2\pi}{t}(y - y_j)\right]}{\cosh\left[\frac{2\pi}{t}(x - x_j)\right] - \cos\left[\frac{2\pi}{t}(y - y_j)\right]}\right) \tag{14}$$

$$c_y(x,y) = w_{y\infty} + \sum_{j=1}^{M} \frac{\gamma(s_j)\Delta s_j}{2t} \left(\frac{\sin\left[\frac{2\pi}{t}(x - x_j)\right]}{\cosh\left[\frac{2\pi}{t}(x - x_j)\right] - \cos\left[\frac{2\pi}{t}(y - y_j)\right]} \right) \tag{15}$$

Overall Program Structure

The goal of the present work is to combine the previously introduced methods (SLC, SEMEL's off-design calculations and surface vorticity) in a single MATLAB program that will allow the computation of all velocity components throughout the channel, with some restrictions regarding the bladed region as described above. The starting point of the program consists in specifying the geometric and operating parameters of an axial fan, including a radial swirl distribution defined herein as

$$rc_{\theta 3} = ar + b \tag{16}$$

in the manner of HORLOCK[11]. With this input, the $c_{\theta 3}$ and c_{z3} radial velocity profiles can be computed from eqs. (4) and (5) depending on the operating point of the machine. The next step, although not mandatory for the SLC iterations, is the calculation of the blade geometry. This is achieved by stacking and interpolating several NACA profile sections which in turn are generated from a 1d-design by inverse calculation as mentioned in the previous section. This is equivalent to the (preliminary) assumption of streamlines parallel to the rotation axis, even though the swirl distribution according to eq. (16) is not necessarily that of a free-vortex fan.

With the known $c_{\theta 3}$ velocity profile and the rough meridional outline of the blade as input, the SLC computing grid is defined and iterations are run until convergence. The SLC output contains the streamline pattern in the S2 plane as shown in Figure 1 and the c_m velocity profiles for each axial computing station. The streamlines are then used to compute an S1 intersection surface with the blade body. This 3D surface is transferred to a 2D plane by means of conformal transformation as described by LEWIS [4] for diagonal flow turbomachines. The generation of a 2D blade section allows the application of the surface vorticity method in order to calculate the cascade flow field on the S1 surface. With these results, further values can be calculated from the computed velocities. From the perspective of the fan design process, three of them are of particular interest, namely the total-to-static (t-s) pressure difference

$$\Delta p_{t-s} = \Delta p_t - \frac{\rho}{2} c_2^2 \tag{17}$$

, the t-s efficiency

$$\eta_{t-s} = \frac{\Delta p_{t-s}}{\Delta p_t} \tag{18}$$

and the slip factor

$$\mu = \frac{c_{\theta 2,real}}{c_{\theta 2,ideal}} \tag{19}$$

The latter is a well-known value in turbomachinery design, expressing the effect of "slip" which means that a real flow will never exactly follow the angle prescribed by the blade shape. In consequence, the actual swirl velocity $c_{\theta 2,real}$ will always be smaller than the design value $c_{\theta 2,ideal}$, thereby reducing the overall performance of the machine. The definition of μ in eq. (19) is taken from DIXON [12] and allows its calculation directly from the blade outlet velocity.

The structure of the final MATLAB program as implemented and used for the calculations presented later can be summarized as follows:

1. Definition of geometric and operating parameters

2. Calculation of $c_{\theta 3}$ and c_{z3} velocity profiles from eqs. (4) and (5)
3. 1D design of blade sections and calculation of blade geometry
4. SLC iterations
5. Calculation of S1 intersection surfaces between streamlines and blade body
6. Conformal transformation of intersection surfaces to 2d plane
7. Computation of S1 velocity field by surface vorticity method
8. Optional postprocessing (graphics, STL files, …)

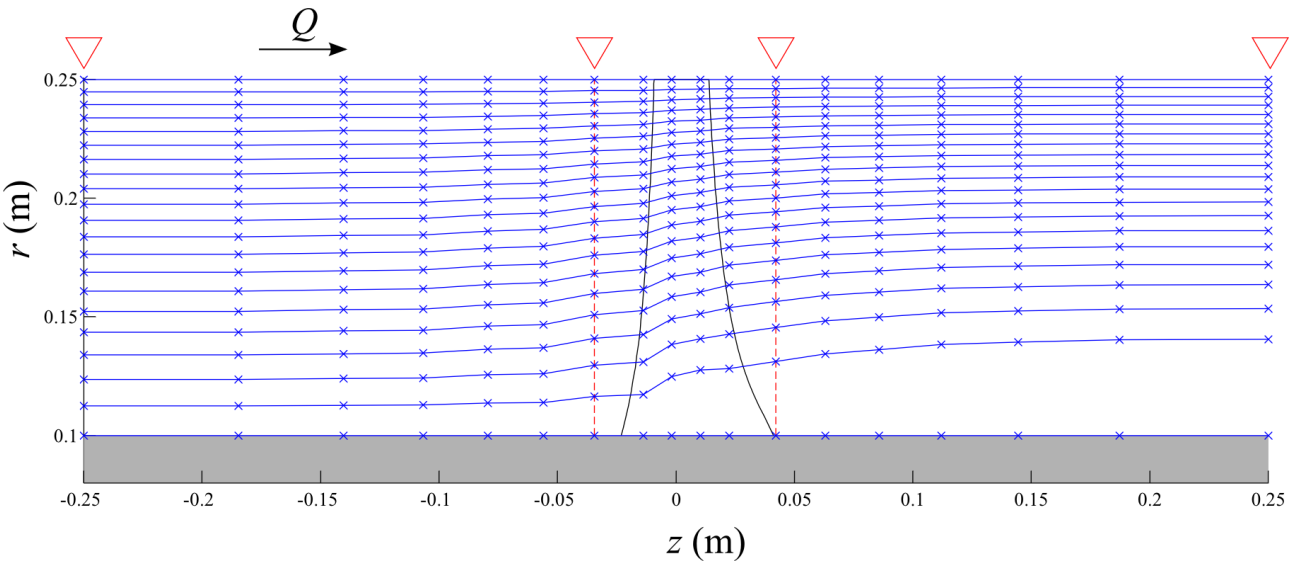

Figure 1: S2 Streamline pattern for χ=0,6 after SLC convergence (triangles mark locations of monitoring planes)

EXPERIMENTAL SETUP

Reference design

The implementation of the program described in the previous chapter was used to perform calculations on a reference fan geometry shown in Figure 2, designed with the parameters listed in Table 1.

Table 1: Parameters of reference fan design

Parameter	**Value**
Tip radius	0,25 m
Hub-to-tip ratio	0,4
Number of blades	13
Revolution speed	3000 min^{-1}
Total pressure rise	1000 Pa
Volume flow	3,5 m^3/s
Swirl parameter a	4 m/s
Swirl parameter b	2,656 m^3/s

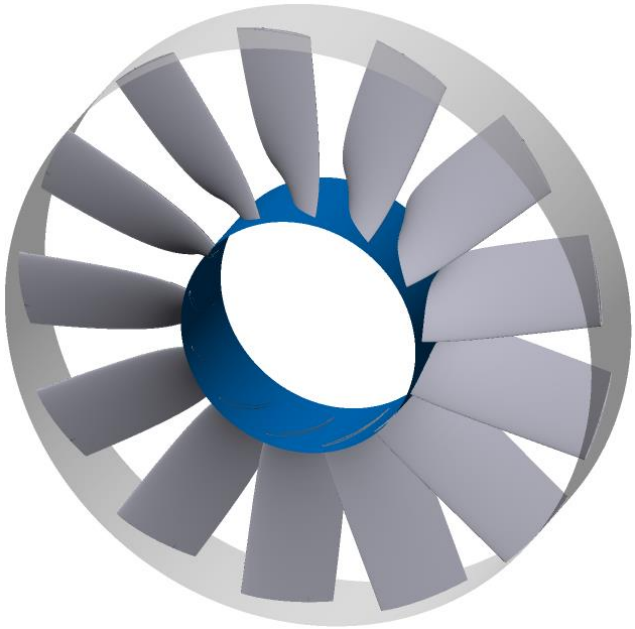

Figure 2: Geometry of reference fan

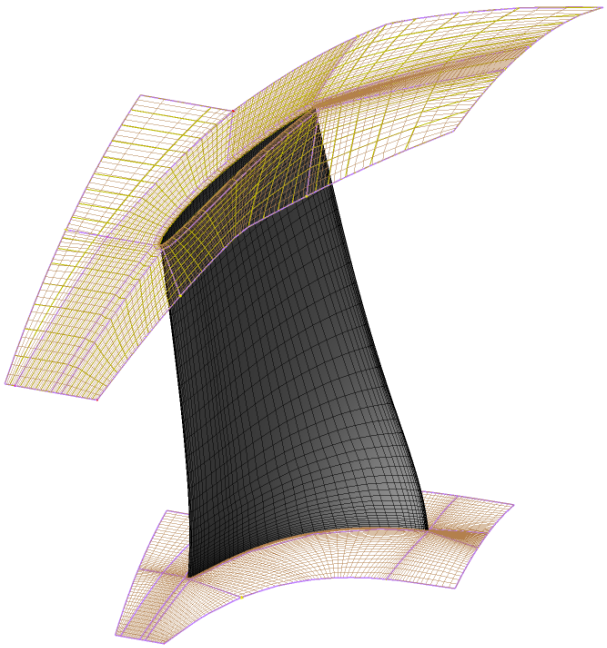

Figure 3: Blade passage meshing

CFD Setup

The validation of the results was carried out by simulating the 3D flow field in the blade passage of the reference fan in the commercial CFD software ANSYS CFX, version 14.5.7. A grid study was performed to ensure the independence of the results from the element size. The size of the used mesh was 743,400 elements. The CFD simulation domain was set up as shown in Figure 4, with a rotating frame of reference for the bladed area which was connected to the stationary frame by two frozen rotor interfaces. No tip gap was set. Velocity and pressure data were monitored at locations 2, 4, 5 and 6; the corresponding monitoring planes (MP) are numbered form 0 to 3. Although the SLC grid only stretched from MP 0 to MP 3 and was thus considerably shorter than the CFD domain, results have later confirmed that radial equilibrium flow conditions were given at MP 0 and 3.

In contrast to the SLC and S1 vorticity calculations, a viscous flow model was used to show the effects of stall and thus the limitations of the implemented model. The wall boundary condition was set to no slip and the turbulence model was shear stress transport (SST). The simulations were carried out both in SLC and CFD for operating points featuring a volume flow ratio χ in the range from 0,6 to 1,5 at intervals of 0,1.

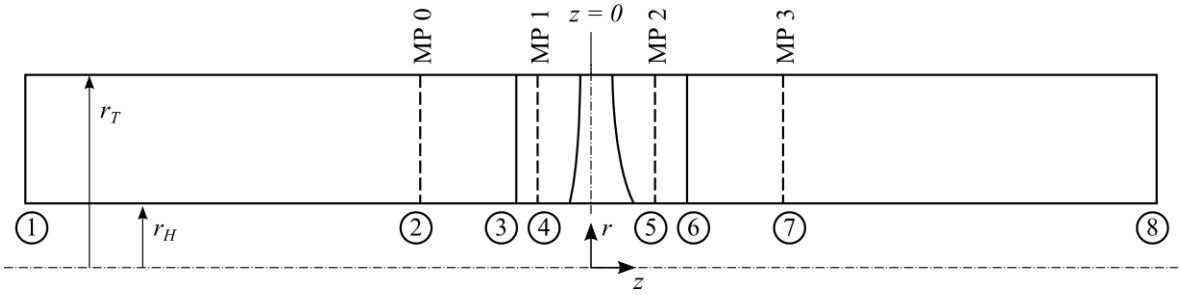

Figure 4: CFD simulation domain and monitoring planes (MP)

Table 2: Axial stations of CFD and SLC setup from Figure 4

Nr.	Designation	z location (m)
1	CFD channel inlet	-0,750
2	SLC channel inlet / monitoring plane 0	-0,250
3	Frozen rotor interface 1	-0,040
4	SLC blade inlet / monitoring plane 1	-0,030
5	SLC blade outlet / monitoring plane 2	0,045
6	Frozen rotor interface 2	0,060
7	SLC channel outlet / monitoring plane 3	0,250
8	CFD channel outlet	0,750

RESULTS AND DISCUSSION

The values for the meridional velocity c_m, the tangential velocity c_θ and the slip factor μ obtained from the implemented program (IMP) and CFD are shown in Figure 5 for the operating points $\chi = 1{,}0$ (design point) and $\chi = 0{,}8$ (partial load), respectively. Additionally, the c_θ curves from predesign (PRE) used as SLC input are also shown for comparison. All values refer to the blade outlet plane (MP 2). Strictly speaking, the c_θ PRE values should only apply to MP 3 but as stated above, swirl is assumed to remain constant from blade outlet (MP 2) to channel outlet (MP 3). The vertical axis is labeled with the blade span r^* ranging from 0 at hub radius to 1 at tip radius.

The IMP and CFD curves show good agreement in general and an almost perfect match for $\chi = 0{,}8$. Major deviations only occur in the c_m velocity profiles at the blade root where effects such as stall and recirculation are not accounted for in the inviscid, stationary flow model and, of course, close to the walls. IMP c_m values range from 18 to 23 m/s for $\chi = 1{,}0$ and from 9 to 21 m/s for $\chi = 0{,}8$ with an increase from hub to tip, respectively. Conversely, c_θ decreases from 28 to 8 m/s along the blade span for $\chi = 1{,}0$ and from 29 to 15 m/s for $\chi = 0{,}8$. As to the swirl velocity, there is a significant difference between the predesign (PRE) values and the IMP/CFD values due to slip. This can directly be observed in the slip factor which starts from values close to 1 at the hub where PRE and IMP c_θ values are relatively close to each other and then falls as the gap between the c_θ curves widens.

With the IMP and CFD calculations performed for χ between 0,6 and 1,5, the Δp_{t-s} and η_{t-s} head curves of the reference fan can be drawn as shown in Figure 6. The Δp_{t-s} values were mass-flow averaged over the channel cross section. Again, an excellent agreement between the two results is observed for $\chi > 0{,}8$. The deviations setting in below this point can again mainly be attributed to stall and recirculation. It is notable that the offset between the PRE and IMP Δp_{t-s} curves is nearly constant. The limits of the simulated operating range are set by the convergence of both SLC and CFD calculations in partial load and by the "inversion" of the turbomachine in overload where the blades do not transfer energy to the fluid anymore but instead act as obstacles causing pressure loss.

In addition, the S1 flow fields around the blade sections over blade span which are also an output of the implemented program have been compared with the CFD results on cylindrical surfaces. Although the compared surfaces are not exactly identical due to streamline curvature, the difference is being neglected here as the comparison can only be qualitative anyway. Figure 7 shows the comparison of the flow fields in the rotating frame at the blade root for $\chi = 1{,}0$. The most obvious difference is the existence of a wake behind the blade in CFD as opposed to the potential flow IMP solution. Otherwise, the velocity data are in good agreement, thus confirming the validation of SMITH [2].

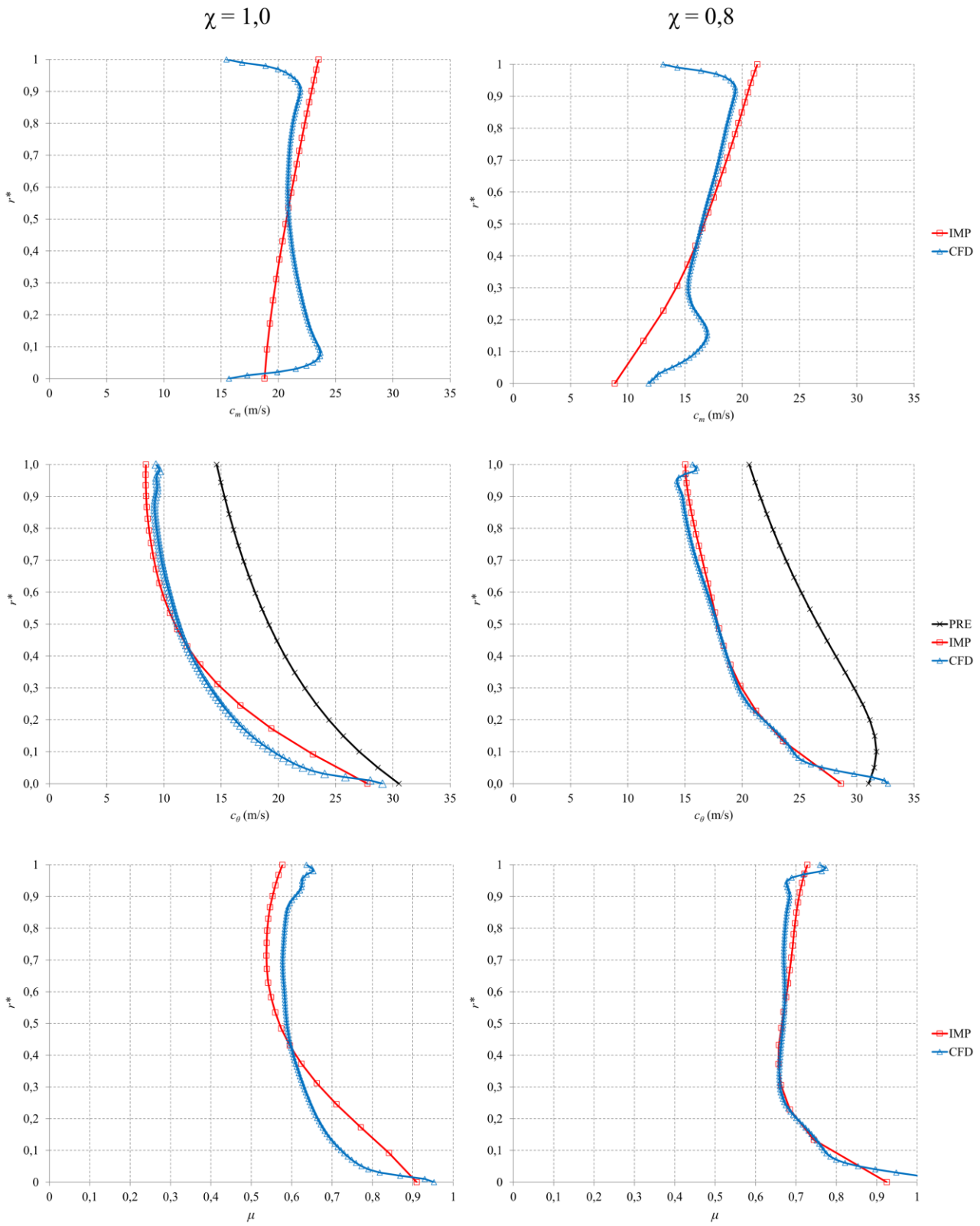

Figure 5: Results from predesign (PRE), implemented program (IMP) and CFD - top to bottom: meridional velocity, swirl velocity, slip factor; left: design point, right: partial load operating point

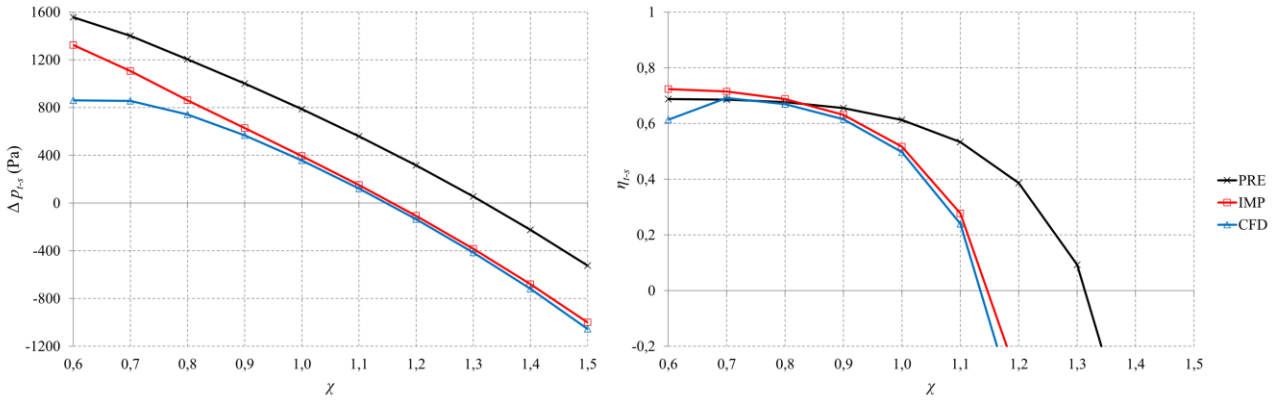

Figure 6: head curves - left: t-s pressure difference, right: t-s efficiency

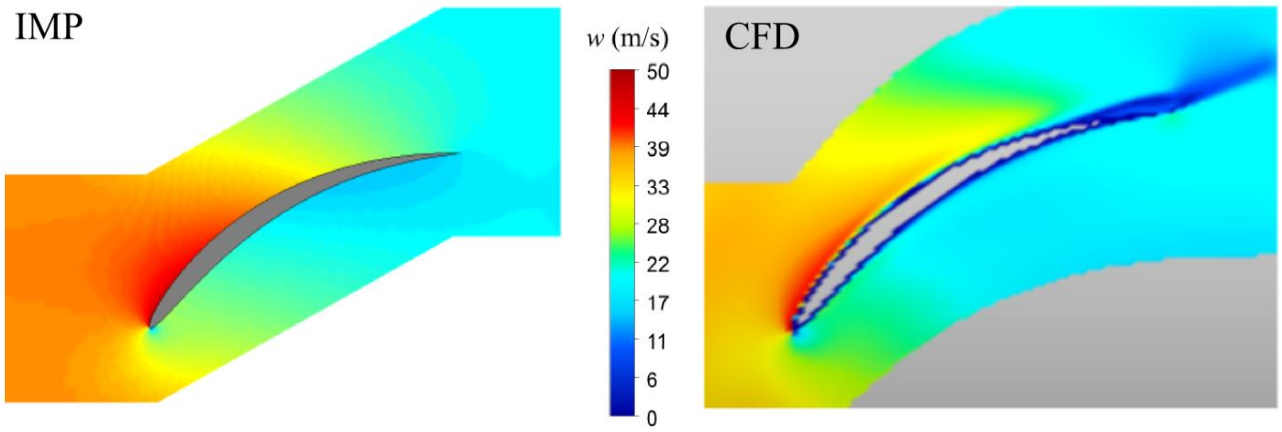

Figure 7: Comparison of relative velocities at blade root section for $\chi = 1{,}0$ – left: surface vorticity method, right: CFD

SUMMARY AND OUTLOOK

A novel procedure has been thought out and implemented in MATLAB with the aim to enable precise calculations of the off-design flow field in an axial fan accounting for the existence of curved meridional streamlines. This has been achieved by combining three existing methods, namely the off-design radial equilibrium calculations by SEMEL, the streamline curvature method in the S2 plane and the surface vorticity method on the S1 surfaces. The velocity and pressure data have been computed throughout the flow channel from inlet to outlet for a range of operating points between $\chi = 0{,}6$ and $\chi = 1{,}5$. The data have been subsequently compared with the corresponding CFD simulations for verification. The results show excellent agreement both in partial load and overload conditions. The new method should thus provide a reliable tool for the design process of axial fans.

A further improvement of the program could include the possibility to use the results as an input for correction of the blade geometry in order to achieve the specified design goal in terms of t-s pressure rise and efficiency, thereby creating a full inverse design routine. Of course, this would require the implementation of another iteration level above the three already existing ones, which presumably would increase the total runtime of the program significantly. The potential of such a procedure lies in the possibility to carry out design or predesign calculations theoretically without any use of CFD, which could save a considerable amount of time and computing resources since it is still common practice to perform iterative loops of CFD simulation and blade geometry corrections.

BIBLIOGRAPHY

[1] H. Smith, M. Semel, P. Epple, M. Miclea-Bleiziffer, A. Delgado – *Accurate Calculation of the Slip Factor of Axial Cascades and Impellers for Arbitrary Blade Shapes.* In: Proceedings of ASME Turbo Expo 2011, Vancouver, Canada, **2011**

[2] H. Smith – *Erweiterung eindimensionaler Auslegungsverfahren für axiale Schaufelgitter durch exakte Berechnung der zweidimensionalen reibungsfreien Strömung*. Diploma thesis, University Erlangen-Nuremberg, **2010**

[3] M. Semel – *Preliminary Design of Axial Fans at Off-design Working Points*. In: Proceedings of ASME Turbo Expo 2014, Düsseldorf, Germany, **2014**

[4] R. I. Lewis – Vortex Element Methods for Fluid Dynamic Analysis of Engineering Systems. Cambridge University Press, New York, **1991**

[5] R. I. Lewis – *Turbomachinery Performance Analysis*. Arnold, London, **1996**

[6] W. Traupel – *Die Berechnung der Potentialströmung durch Schaufelgitter*. Technische Rundschau Sulzer, 1(1): p. 25-42, **1945**

[7] R. A. Novak – *Streamline Curvature Computing Procedures for Fluid-Flow Problems*. J. Eng. Power, 89(4): p. 478-490, **1967**

[8] B. Lakshminarayana – *Fluid Dynamics and Heat Transfer of Turbomachinery*. John Wiley & Sons, New York, **1996**

[9] R. M. Hearsey – *Practical Compressor Aerodynamic Design*. In: Advanced Topics in Turbo-machinery Technology, Concepts ETI, Inc., **1986**

[10] M. T. Schobeiri – *Turbomachinery Flow Physics and Dynamic Performance*, 2nd edition. Springer, **2012**

[11] J. H. Horlock – *Axial Flow Compressors*. Butterworths Publications Limited, London, **1958**

[12] S. L. Dixon, C. A. Hall - *Fluid Mechanics and Thermodynamics of Turbomachinery*, 6th edition. Butterworth-Heinemann, **2010**

ANNEX

Nomenclature

Variables	
a, b	Swirl parameters
C	Abbreviating coefficient
c	Absolute streaming velocity
F	Body forces
h	enthalpy
K, k	Coupling coefficients
n	exponent
M	Number of panels
p	pressure
Q	Volumetric flow
r	Radial coordinate
μ	Slip factor
ρ	air density
ϕ	Slope angle (streamline)
χ	Volume flow ratio
ψ	Local head coefficient
ω	Angular revolution speed

Subscripts	
0	Channel inlet
1	Blade inlet
2	Blade outlet
3	Channel outlet

s	Curvilinear surface coordinate	∞	Infinite distance
T	Temperature	c	Curvature
t	Blade spacing	i, j	Counting indices
w	Relative streaming velocity	m	Meridional
x, y, z	Cartesian coordinates	n	Normal
α	Angle of attack	s	Static
β	Relative streaming angle	t	Total
γ	Local vorticity strength	$t-s$	Total-to-static
η	Efficiency	op	Operating
ϑ	Slope angle (airfoil outline)	des	Design
θ	Tangential direction		